ATMOSPHERIC AND OCEANIC SCIENCE LETTERS, 2013, VOL. 6, NO. 4, 203–209

The Long-Term Field Experiment Observatory and Preliminary Analysis of Land-Atmosphere Interaction over Hilly Zone in the Subtropical Monsoon Region of Southern China

LIU Jian-Guo[1,2], XIE Zheng-Hui[1], JIA Bing-Hao[1], TIAN Xiang-Jun[1], QIN Pei-Hua[1], ZOU Jing[1,2], YU Yan[1,2], SUN Qin[1,2], WANG Yuan-Yuan[1,2], XIE Jin-Bo[1,2], and XIE Zhi-Peng[1,2]

[1] *State Key Laboratory of Numerical Modeling for Atmospheric Sciences and Geophysical Fluid Dynamics (LASG), Institute of Atmospheric Physics, Chinese Academy of Sciences, Beijing 100029, China*
[2] *University of Chinese Academy of Sciences, Beijing 100049, China*

Received 24 January 2013; revised 17 March 2013; accepted 7 April 2013; published 16 July 2013

Abstract To improve current understanding of the water cycle, energy partitioning and CO_2 exchange over hilly zone vegetative land surfaces in the subtropical monsoon environment of southern China, a long-term field experiment observatory was set up at Ningxiang, eastern Hunan Province. This paper presents a preliminary analysis of the field observations at the observatory collected from August to November 2012. Results show that significant diurnal variations in soil temperature occur only in shallow soil layers (0.05, 0.10, and 0.20 m), and that heavy rainfall affects soil moisture in the deep layers ($\geqslant$ 0.40 m). During the experimental period, significant diurnal variations in albedo, radiation components, energy components, and CO_2 flux were observed, but little seasonal variation. Strong photosynthesis in the vegetation canopy enhanced the CO_2 absorption and the latent heat released in daylight hours; Latent heat of evaporation was the main consumer of available energy in late summer. Because the field experiment data are demonstrably reliable, the observatory will provide reliable long-term measurements for future investigations of the land-atmosphere interaction over hilly land surfaces in the subtropical monsoon region of southern China.

Keywords: field observation, subtropical monsoon region, hilly zone, surface flux, land-atmosphere interaction
Citation: Liu, J.-G., Z.-H. Xie, B.-H. Jia, et al., 2013: The long-term field experiment observatory and preliminary analysis of land-atmosphere interaction over Hilly Zone in the subtropical monsoon region of southern China, *Atmos. Oceanic Sci. Lett.*, **6**, 203–209, doi:10.3878/j.issn.1674-2834.13.0112.

1 Introduction

Land surface processes play an important role in the global water cycle, energy balance, and the budget of greenhouse gases (such as CO_2) by controlling the exchanges of energy and mass fluxes between the land-surface and the atmosphere (Intergovernmental Panel on Climate Change (IPCC), 1995). Understanding these land-atmospheric flux exchanges is a crucial topic in climate change research. Climate simulations are especially sensitive to the surface partitioning of available energy into sensible and latent heat fluxes (Rowntree, 1991; Dickinson et al., 1991). To better understand the water cycle, energy partitioning and CO_2 exchange, researchers across the globe have conducted many field studies in recent decades, over diverse terrestrial surfaces such as forests, grasslands, and paddy fields (Baldocchi and Vogel, 1997; Toda et al., 2002; Gao et al., 2003). Throughout the past 30 years, numerous field studies have been also been performed in the arid and semi-arid regions of northern China, including Inner Mongolia (Lu et al., 2002, 2005; Gao et al., 2009), the Heihe River basin (Wang and Mitsuta, 1991, 1992; Hu, 1994; Hu and Gao, 1994), Dunhuang (Zhang and Shuangguan, 2002), Loess Plateau (Wang et al., 2010), and Tongyu (Liu et al, 2004, 2006).

Land-atmosphere interactions in the monsoon environment have recently received considerable attention, and several field experiments have been conducted in these regions (Toda et al., 2002; Song et al., 2004; Barros et al., 2005; Bi et al., 2007; Gao et al., 2009; Li et al., 2009). However, little attention has been devoted to long-term measurements over the hilly zone, one of the most important terrestrial ecosystems in the subtropical monsoon environment of southern China. To fill this gap, a long-term field experimental observatory for assessing land-atmosphere interactions was constructed at Ningxiang (eastern Hunan Province, southern China) in August 2012, by the State Key Laboratory of Numerical Modeling for Atmospheric Sciences and Geophysical Fluid Dynamics (LASG), Institute of Atmospheric Physics (IAP), the Chinese Academy of Sciences (CAS). The main aims of the observatory are to: (1) monitor the water table; (2) monitor the long-term trends in subtropical monsoon climate changes; (3) study the land-atmosphere interaction over this area; (4) improve existing land surface and climate models. Continuous and long-term observations over the hilly zone in the subtropical monsoon environment of southern China will be undertaken in future.

The present work briefly introduces the observatory at Ningxiang, and presents a preliminary analysis of the field observations collected from August to November 2012.

2 Field experiment observatory

2.1 Site

Since 10 August 2012, micrometeorological measure-

Corresponding author: XIE Zheng-Hui, zxie@lasg.iap.ac.cn

ments have been conducted at a hilly zone experimental site (28°20'N, 112°34'E), approximately 4 km from Ningxiang county and about 36 km from Changsha City (hereafter, this site is referred to as Ningxiang observatory), based in eastern Hunan Province in the subtropical monsoon region of southern China (Fig. 1a). The site terrain is relatively flat with a homogenous underlying surface. The site is surrounded by similar vegetation, mainly evergreen broadleaved forest and shrub, and some secondary vegetation. The average height of vegetation is approximately 7 m. The soil is predominantly red soil with rapid drainage of water (Figs. 1b, 1d, and 1e).The average elevation is approximately 110 m, annual mean temperature is 16.8°C, annual mean rainfall is 1358 mm, average relative humidity is 81%, and annual average sunshine is 1739.2 hours. The micrometeorological measurement sensors are installed in a measurement tower of height 20 m. Figure 1 shows the location and site of the observatory and its main measurement instruments, taken on 9 August 2012.

The various instruments at the observatory measure: (1) water table depth (at nine different wells surrounding the measurement tower); (2) heat and water content of soil; (3) boundary layer meteorological parameters; (4) surface radiation; and (5) surface flux.

2.2 Micrometeorological measurements

The principle micrometeorological instruments at Ningxiang observatory comprise: (1) a surface layer meteorology observation system; (2) a radiation flux observation system; (3) an eddy covariance system (EC); and (4) a soil temperature/humidity measuring system.

Surface meteorological measurements include wind speed and direction (WindSonic1405-PK052, Gill), and air temperature and relative humidity (HMP155A-L, Vaisala) at 9.5 and 13.5 m above the ground (Fig. 1c). Barometric pressure is measured with a CS106 Barometric Pressure Sensor (Vaisala) over a 500 to 1100 hPa range. Precipitation is measured by a tipping bucket Rain Gauge (TE525MM-L, Texas Electronics) at 0.1 mm increments mounted at 20 m on the tower. These signals are logged to a data logger (CR1000, Campbell) and recorded every 10 min.

The surface radiation system observes upward and downward short-wave radiation (UR and DR), and upward and downward long-wave radiation (ULR and DLR). Radiation is intercepted by a 4-Component Net Radiation Sensor (CNR4, Kipp & Zonen) mounted at a height of 17.5 m (Fig. 1c). The data are recorded by a Datataker (CR3000, Campbell) equipped with a memory card. The data are sampled each minute and averaged every 30 min.

The eddy covariance instruments include a three-dimensional sonic anemometer (CSAT3, Campbell) and an open path infrared CO_2 and H_2O analyzer (EC150, Campbell). The CSAT3 points toward the prevailing wind direction and measures the means and standard deviations of the wind velocity components (i.e., u, v, and w) and air temperature (T). The EC150 measures the means and standard deviations of water vapor density and CO_2. Sensor outputs are recorded at a sampling rate of 10 Hz, averaged over 30 min periods, and logged to the above-mentioned data logger. The sensors are installed on a tower 17.5 m above the ground (Fig. 1d). The momentum, latent, and sensible heat fluxes are calculated by the eddy covariance method. The turbulent fluxes are post-field data processed by a set of necessary correlation procedures, such as coordinate rotation by the planar fits method (PF) (Wilczak et al., 2001), frequency response correction (Moore, 1986), sonic temperature correction (Schotanus et al, 1983), and density flux correction accounting for density effects due to heat and water vapor fluctuations (WPL correction, Webb et al., 1980).

Soil moisture and temperature are measured with a water content reflectometer (CS616-L, Campbell) and a soil temperature profile sensor (109-L, Campbell) respec-

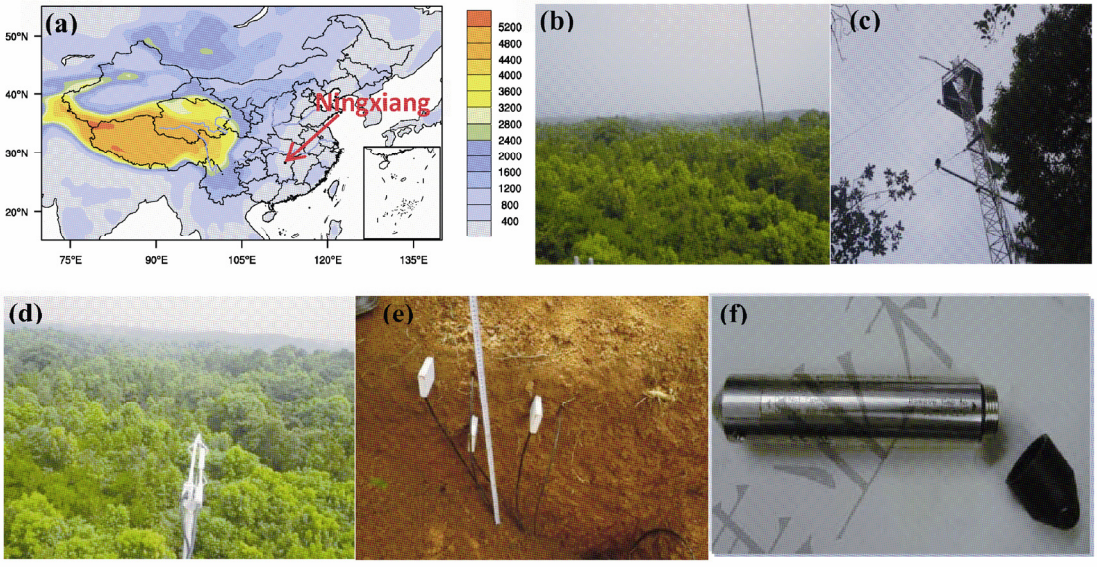

Figure 1 Ningxiang field experiment observatory: (a) location and elevation; (b) underlying canopy surface; (c) measurement tower; (d) EC 150 sensor and underlying surface; (e) soil temperature and moisture sensors and their site; (f) water table depth sensor.

tively (Fig. 1e). These instruments sample at seven soil depths (0.05, 0.10, 0.20, 0.40, 0.60, 0.80, and 1.00 m). To complete the surface energy balance, soil heat flux is measured by a heat flux plate (HFP01-L50, Campbell) embedded 0.05 m deep in the soil (this instrument was installed 16 November 2012). The data are recorded at 10 min intervals by a Datataker (CR1000, Campbell) with a memory card.

2.3 Water table depth measurement

The main instrument for water table measurement at Ningxiang observatory is the HOBO U20 series water table sensor, which includes data loggers (U20, Onset; see Fig. 1f) placed in nine different wells, connected to a computer through a Universal Optic-USB Base station (BASE-U-4, Onset). Data from the HOBO loggers are launched, read out and plotted by HOBO ware Pro software (BHW-PC, Onset).

3 Preliminary results

To examine the reliability of measurement data from Ningxiang observatory, we conducted a preliminary analysis of the field data collected from 10 August to 16 November 2012. We investigated the diurnal and seasonal variation of near-surface meteorology elements, soil moisture and soil temperature, radiation and energy components, CO_2 fluxes, and water table depth.

3.1 Variation of near surface meteorology elements and water table depth

Figures 2a–d show the temporal variations in daily average wind direction (WD), wind speed (WS), air temperature (T), and relative humidity (RH) at heights of 9.5 m and 13.5 m. Figures 2e–f present the air pressure and daily total rainfall at Ningxiang observatory. As shown in Figs. 2a–d, the daily mean WD and WS at 9.5 m (225.9° and 0.91 m s^{-1}, respectively) is slightly less than at 13.5 m (245.3° and 1.39 m s^{-1}, respectively). The variability in these quantities is very similar at both heights (R_{WD}=0.87, R_{WS}=0.97 at 9.5 and 13.5 m, respectively, where R denotes the correlation coefficient). The maximum daily mean wind speed on 29 September 2012 was 1.89 m s^{-1} at 9.5 m and 2.69 m s^{-1} at 13.5 m. The air temperature and relative humidity at 9.5 m (T_{mean}= 21.73°C, RH_{mean}= 80.77%) are essentially the same at 13.5 m (T_{mean}= 21.88°C, RH_{mean}=80.09%, R_T=1, R_{RH}=1). The air temperature varied significantly with season (from late summer to autumn). The daily mean air temperature (at 9.5 m) reached a maximum (31.3°C) on 20 August, while the lowest air temperature (12.55°C) was recorded on 5 November 2012. Seasonal variation was also observed in air pressure (P) (P_{max} = 1013 hPa; P_{min} = 991 hPa), and was significant negatively correlated with T (R = –0.9). Figure 2 displays typical subtropical monsoon climate characteristics at this time of year. The water table depth ranged 4–6 m (data not shown).

3.2 Variation of soil temperature and soil moisture

Near-surface soil moisture and soil temperature control the partitioning of energy in latent and sensible heat fluxes at the soil-atmosphere interface (Albergel et al., 2012). Figure 3a plots the temporal variation of daily mean air temperature, while Figs. 3b and 3c show the temporal and

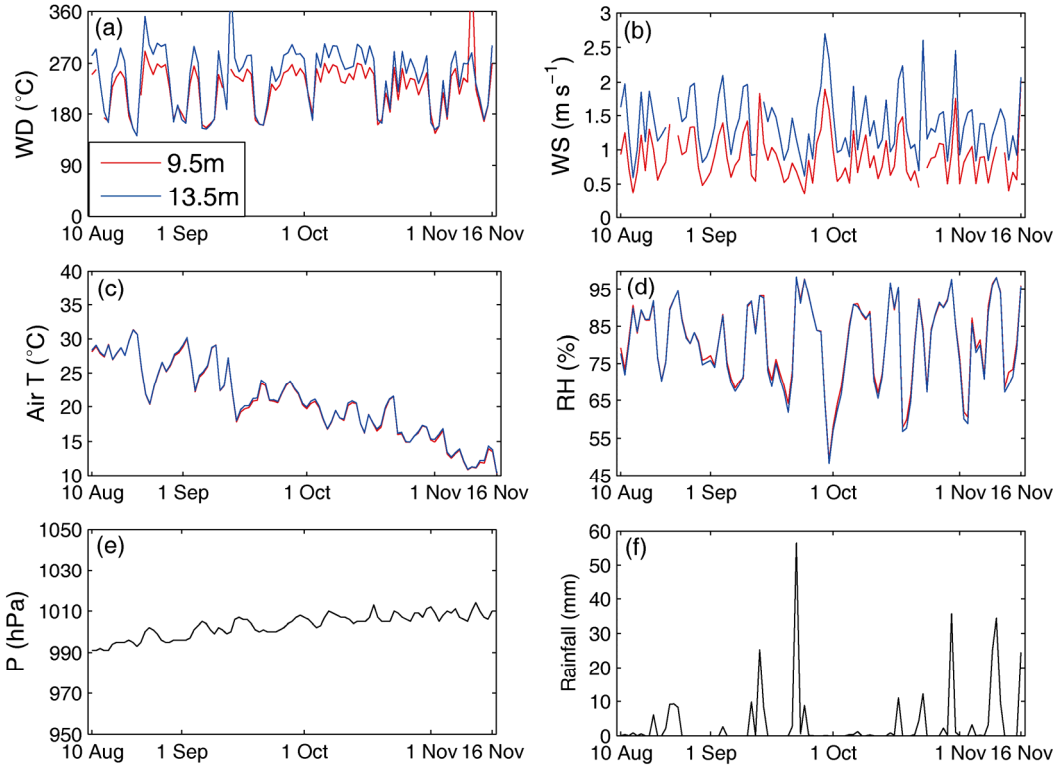

Figure 2 Meteorological data collected at Ningxiang observatory at 9.5 m (red) and 13.5 m (blue) from 10 August to 16 November 2012: (a) Wind Direction (WD); (b) Wind Speed (WS); (c) Air Temperature (Air T); (d) Relative Humidity (RH); (e) Air Pressure (P); (f) Rainfall (daily).

diurnal variation of soil temperature at depths of 0.05, 0.10, 0.20, 0.40, 0.60, 0.80 and 1.00 m. Figure 3d shows the variation of daily total rainfall, while the temporal and diurnal variations of soil moisture at the abovementioned depths are plotted in Figs. 3e–f.

The temporal variation trends of soil and air temperatures are similar, especially in the shallow layers ($R_{0.05\,m}$ = 0.97, $R_{0.10\,m}$ = 0.95, and $R_{0.20\,m}$ = 0.93). Soil temperature changed seasonally in each soil layer. These changes were significant in shallow layers and weakened with increasing depth (Figs. 3a–b); the maximum standard deviation (SDV, 4.10°C) occurred at depth 0.05 m, while the lowest (1.79°C) was recorded at 1.00 m. Soil temperature showed significant diurnal variation in shallow layers, but almost no diurnal variation in deeper layers ($\geqslant$ 0.40 m; see Fig. 3c).

In each layer, soil moisture was strongly affected by rainfall. Significant differences occurred after a heavy rainfall even in deep layers (e.g., 22 September, 30 October, and 10–11 November, see Figs. 3d–e). Dramatic diurnal changes in deep-layer soil moisture after heavy rainfall are evident in Fig. 3f. Figures 3e and 3f also show negligible seasonal and diurnal variation in soil moisture at 0.20 m (SDV = 0.009 $m^3\ m^{-3}$; SDV > 0.3 $m^3\ m^{-3}$ at other depths); this anomaly is attributable to the soil texture at this depth over the study area.

3.3 Variation of radiation and energy components

Figure 4 plots the temporal and diurnal variation of 30-min means of albedo (Figs. 4a and 4b), radiation components (DR, UR, DLR, and ULR; Figs. 4c and 4d), and energy components (net radiation (RN), sensible heat flux (H), and latent heat flux (LE); Figs. 4e and 4f). Measurements of soil heat flux, which were started on 16 November, are not shown. The albedo of the underlying surface is the ratio of the maximum UR to maximum DR. The RN was calculated from four radiation components. As shown in Figs. 4b, 4d, and 4f, the diurnal courses of radiation and energy components were similar on three days in late summer (25–27 August 2012), and displayed significant variation. The maximum RN, DR, LE, and H (789.6 W m^{-2}, 936.1 W m^{-2}, 411.8 W m^{-2}, and 253.7 W m^{-2}, respectively) occurred at noon of 26 August. LE of evaporation was the main consumer of available energy in late summer. The diurnal variations of RN, DR, and LE were generally consistent (R (DR, LE) = 0.968, R (RN, LE) = 0.967, R (RN, DR) = 0.998). In Figs. 4a, 4c, and 4e, we observe little seasonal variation in albedo, radiation components, and energy components throughout the ex- perimental period. These quantities adequately character-

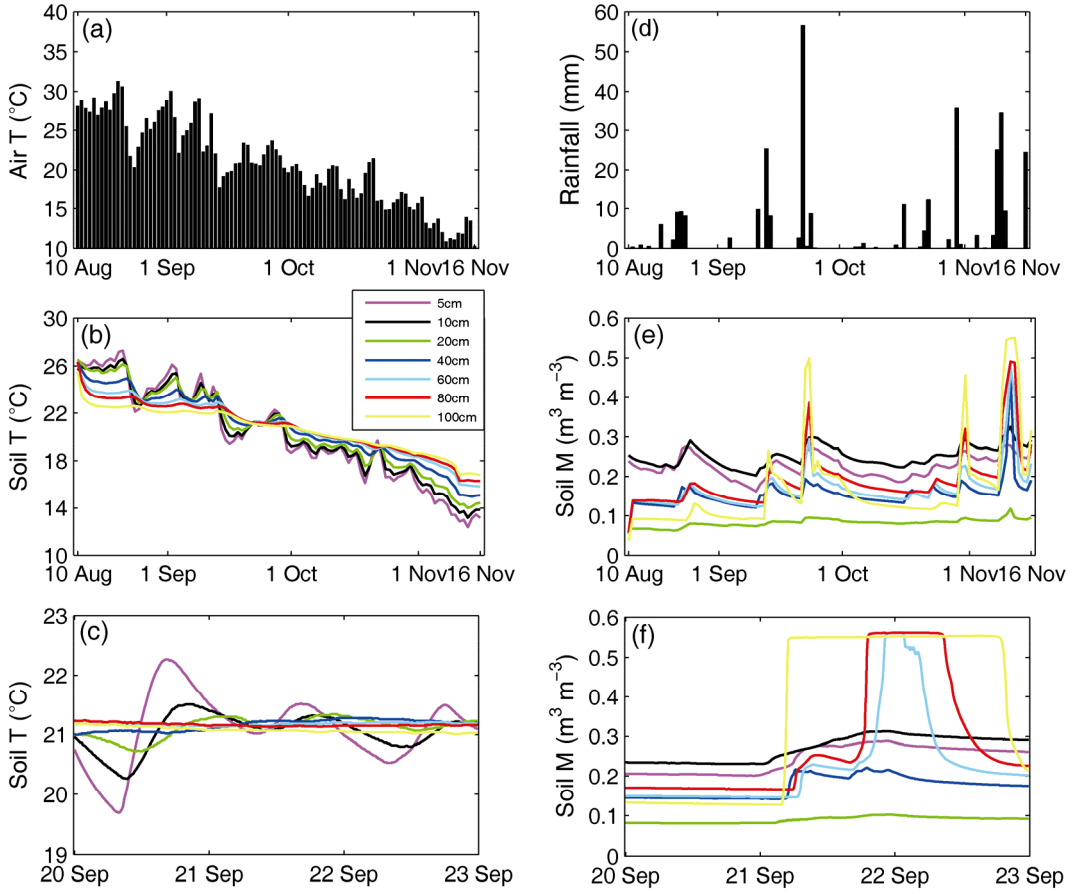

Figure 3 (a) Temporal variation of daily mean Air T; (b–c) Temporal variation (daily mean) and diurnal variation (10 min intervals) of soil temperature (Soil T)at depths of 0.05 (pink), 0.10 (black), 0.20 (green), 0.40 (dark blue), 0.60 (sky blue), 0.80 (red), and 1.00 m (yellow); (d) Temporal variation of daily total rainfall; (e–f) Temporal variation (daily mean), diurnal variation (10 min intervals) of soil moisture(Soil M) at the depths given in (b–c).

ize the energy partition on the vegetation canopy over hilly zones in the subtropical monsoon region of Southern China.

3.4 Variation of CO_2 flux

The CO_2 flux is obtained from the WPL correction (Webb et al., 1980). Noise and other interference is eliminated from 30 minute observations by imposing the criterion $F(t) < (\overline{F} - 4\sigma)$ or $F(t) > (\overline{F} + 4\sigma)$, where $F(t)$ is the observation, $\overline{F}$ is the mean, and σ is SDV over the interval. Figure 5 shows the temporal and diurnal variation of 30-min means of CO_2 flux (negative fluxes indicate CO_2 absorption by vegetation). As shown in Fig. 5b, the diurnal course of CO_2 flux was similar on three days in late summer (25–27 August 2012). Diurnal variation was evident during this time, and the maximum daytime CO_2 flux absorbed by the vegetation canopy reached ~ 1.30 mg m^{-2} s^{-1} on 26 August 2012. The maximum CO_2 flux released during the night was ~ 0.75 mg m^{-2} s^{-1} on 27 August 2012. These results are consistent with those reported by Song et al. (2004). CO_2 flux exhibits little seasonal variation throughout the experimental period, which covers neither the growing season nor the winter season (Fig. 5a). The vegetation canopy comprised the underlying surface, and the mean CO_2 flux was negative (–0.1 mg m^{-2} s^{-1}) during the entire experimental period. These results are attributable to photosynthesis in the vegetation canopy, which is especially active in late summer, and which increases the CO_2 absorption and the LE released in the daylight. As shown in Figs. 4f and 5b, the diurnal variations of LE and CO_2 flux were generally consistent, but in reverse phase (R as high as –0.94).

4 Summary and conclusion

The long-term field experimental observatory at Ningxiang, eastern Hunan Province, was constructed to investigate land-atmosphere interactions, the water cycle, energy balance, and CO_2 exchange over the hilly zone vegetation land-surface in the subtropical monsoon climate environment. The reader has been briefly introduced to the observatory. As a preliminary study, the temporal variation of near-surface meteorology elements, soil moisture and temperature, radiation and energy components, CO_2 fluxes, and water table depth were analyzed during the period 10 August to 16 November 2012 (late summer to autumn). Throughout this period, the near-surface meteorology elements displayed typical subtropical monsoon climate characteristics, with some seasonal variability in air temperature and pressure. Significant diurnal variation in soil temperature was observed at shallow layers (0.05, 0.10, and 0.20 m), while soil moisture was significantly increased after heavy rainfall, even in the deep layers ($\geqslant$ 0.40 m). Albedo, radiation components, energy components, and CO_2 flux showed significant diurnal variation,

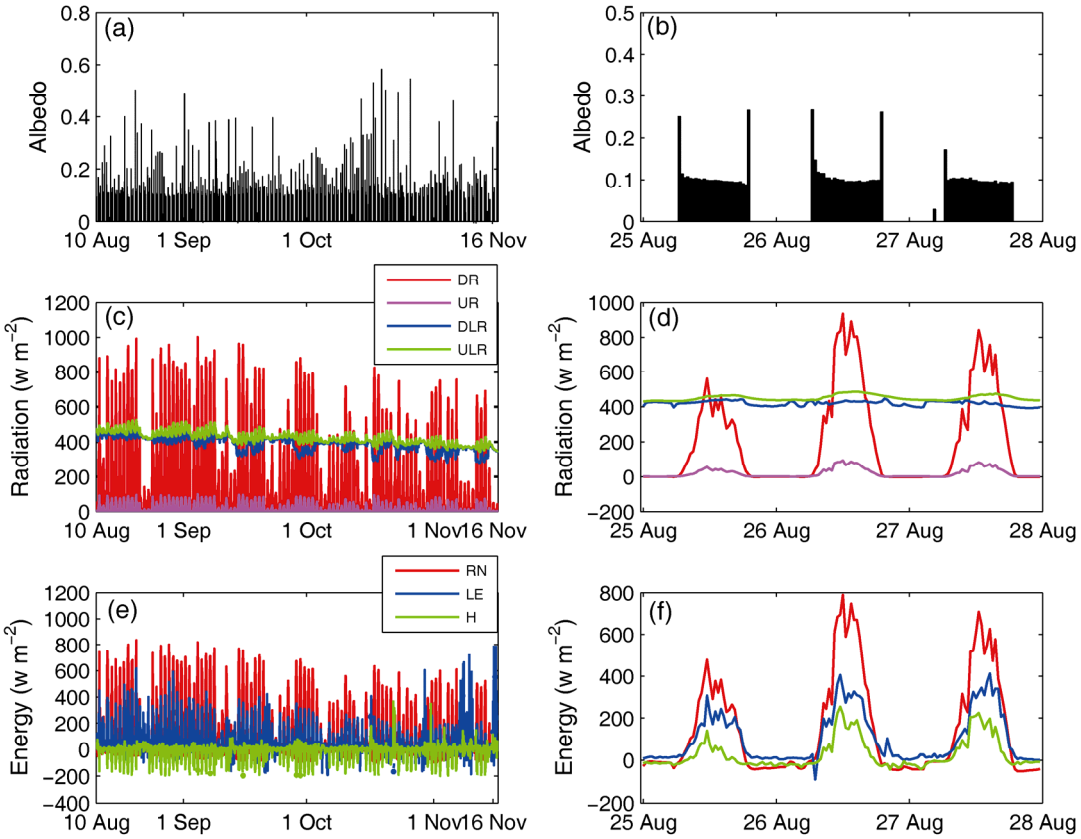

Figure 4 Temporal variation and diurnal variation of (a–b) albedo; (c–d) radiation components (DR (red), UR(pink), DLR (dark blue), ULR (green); (e–f) energy components (RN (red), LE (dark blue), H (green); 30 min intervals).

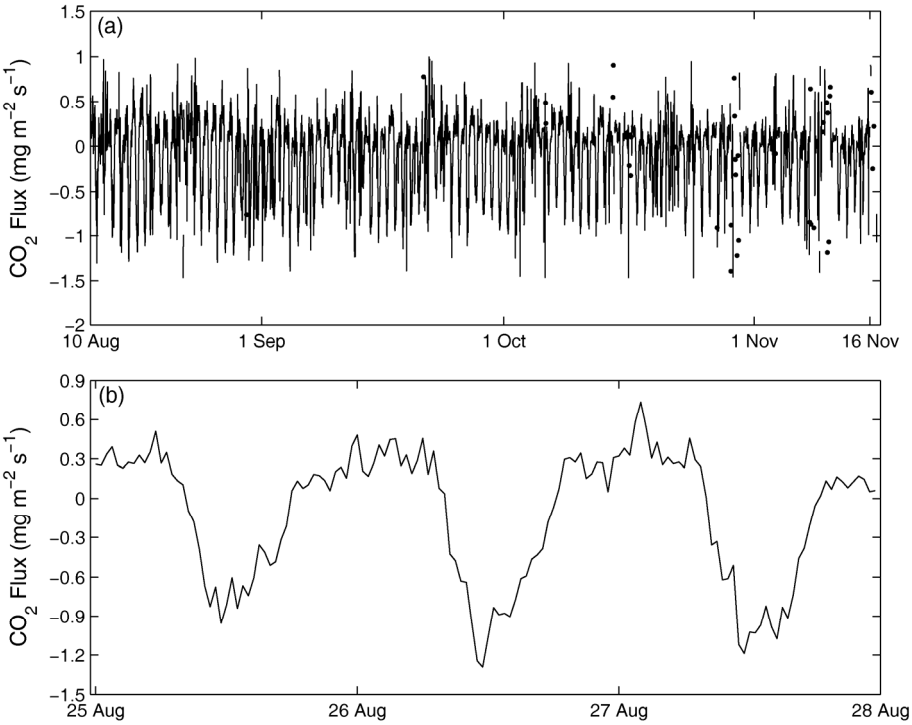

Figure 5 (a) Temporal variation and (b) diurnal variation of CO_2 flux (30 min intervals).

but little seasonal variation. Strong photosynthesis in the vegetation canopy led to enhance CO_2 absorption and the larger LE released during daylight hours. Latent heat flux of evaporation was the main consumer of available energy in late summer.

Preliminary results show that the data acquired by the field experimental observatory are reliable. The observatory will collect long-term measurement data for further investigating the land-atmosphere interactions. The analysis of these long-term data will improve our understanding of the water cycle, energy balance, and CO_2 exchange in the subtropical monsoon climate environment, and will provide better estimates of the key land-surface parameters in atmospheric numerical models.

Acknowledgements. This study was jointly supported by the Strategic Priority Research Program of Chinese Academy of Sciences (Grant No. XDA05110102), the National Natural Science Foundation of China (Grant No. 41075062), and the National Basic Research Program of China (Grant No. 2010CB951001). The authors gratefully acknowledge Professor LIU Hui-Zhi and Professor LI Ai-Guo at IAP, CAS, for their constructive suggestion on the Ningxiang observatory. We are very grateful to the anonymous reviewers for their careful review and valuable comments, which have substantially improved this manuscript.

References

Albergel, C., P. de Rosnay, G. Balsamo, et al., 2012: Soil moisture analyses at ECMWF: Evaluation using global ground-based in situ observations, *J. Hydrometeorol.*, **13**, 1442–1460, doi:http://dx.doi.org/10.1175/JHM-D-11-0107.1.

Baldocchi, D. D., and C. A. Vogel, 1997: Seasonal variation of energy and water vapor exchange rates above and below a boreal jack pine forest canopy, *J. Geophys. Res.*, **102**(D24), 28939–28951.

Barros, A. P., F. Munoz, A. W. Wood, et al., 2005: *Monitoring the Diurnal Cycle of Land-Atmosphere Interactions in Sonora*, Mexico during NAME/SMEX04, 19 AMS Conference on Hydrology, 20pp.

Bi, X., Z. Gao, X. Deng, et al., 2007: Seasonal and diurnal variations in moisture, heat, and CO_2 fluxes over grassland in the tropical monsoon region of southern China, *J. Geophys. Res.*, **112**, D10106, doi:10.1029/2006JD007889.

Dickinson, R. E., A. Hendersin-Sellers, C. Rosenzweig, et al., 1991: Evapotranspiration models with canopy resistance for use in climate models, a review, *Agric. Forest Meteor.*, **54**, 373–388.

Gao, Z., L. Bian, and X. Zhou, 2003: Measurements of turbulent transfer in the near-surface layer over a rice paddy in China, *J. Geophys. Res.*,**108**(D13), 4387, doi:10.1029/2002JD002779.

Gao, Z., D. H. Lenschow, Z. He, et al., 2009: Seasonal and diurnal variations in moisture, heat and CO_2 fluxes over a typical steppe prairie in Inner Mongolia, China, *Hydrol. Earth Syst. Sci.*, **6**, 1939–1972, doi:10.5194/hessd-6-1939-2009.

Hu, Y., 1994: Research advance about the energy budget and transportation of water vapor in the HEIFE area, *Adv. Earth Sci.* (in Chinese), **9**, 30–34.

Hu, Y., and Y. Gao, 1994: Some new understandings of processes at the land surface in arid area from the HEIFE, *Acta Meteor. Sinica* (in Chinese), **52**, 285–296.

IPCC, 1995: Climate Change, in: *The Science of Climate Change*, J. T. Houghton et al. (Eds.), Cambridge University Press, Cambridge and New York, 55–64.

Li, Y. J., L. Zhou, Z. Z. Xu, et al., 2009: Comparison of water vapour, heat and energy exchanges over agricultural and wetland ecosystems, *Hydrol. Process.*, **23**, 2069–2080, doi:10.1002/hyp.7339.

Liu, H., W. Dong, C. Fu, et al., 2004: The long term field experiment on aridification and the ordered human activity in semi-arid area at Tongyu, northeast China, *Climatic Environ. Res.* (in Chinese), **9**, 352–378.

Liu, H., G. Tu, W. Dong, et al., 2006: Seasonal and diurnal variations of the exchange of water vapor and CO_2 between the land surface and atmosphere in the semi-arid area, *Chinese J. Atmos. Sci.* (in Chinese), **30**(1), 108–118.

Lu, D., Z. Chen, J. Chen, et al., 2002: Composite study on Inner Mongolia semiarid grassland soil-vegetation atmosphere interaction (IMGRASS), *Earth Sci. Front* (in Chinese), **9**, 52–63.

Lu, D., Z. Chen, J. Chen, et al., 2005: Study on soil-vegetation-atmosphere interaction in Inner Mongolia semiarid grassland, *Acta Meteor. Sinica* (in Chinese), **63**, 33–55.

Moore, C. J., 1986: Frequency response corrections for eddy correlation systems, *Bound.-Layer Meteor.*, **37**, 17–35, doi:10.1007/BF00122754.

Rowntree, P. R., 1991: Atmospheric parameterization schemes for evaporation over land: Basic concepts and climate modeling aspects, in: *Land Surface Evaporation. Measurement and Parameterization*, T. J. Schmugge and J. C. Andre (Eds.), 5–29, Springer, New York, 5–29.

Schotanus, P., F. T. M. Nieuwstadt, and H. A. R. De Bruin, 1983: Temperature measurement with a sonic anemometer and its application to heat and moisture fluctuations, *Bound.-Layer Meteor.*, **26**, 81–93, doi:10.1007/BF00164332.

Song, X., Y. Liu, X. Xu, et al., 2004: Comparison study on carbon dioxide, water and heat Fluxes of the Forest ecosystem in red earthhilly zone over winter and spring, *Resour. Sci.*, **26**(3), 96–103.

Toda, M., K. Nishida, N. Ohte, et al., 2002: Observations of energy fluxes and evapotranspiration over terrestrial complex land covers in the tropical monsoon environment, *J. Meteor. Soc. Japan*, **80**(3), 465–484.

Wang, G., J. Huang, W. Guo, et al., 2010: Observation analysis of land-atmosphere interactions over the Loess Plateau of northwest China, *J. Geophys. Res.*, **115**, D00K17, doi:10.1029/2009JD 013372.

Wang, J. M., and Y. Mitsuta, 1991: Turbulence structure and transfer characteristics in the surface layer of the HEIFE Gobi area, *J. Meteor. Soc. Japan*, **69**, 587–593.

Wang, J. M., and Y. Mitsuta, 1992: Evaporation from the desert: Some preliminary results of HEIFE, *Bound.-Layer Meteor.*, **59**, 413–418, doi:10.1007/ BF02215461.

Webb, E. K., G. I. Pearman, and R. Leuning, 1980: Correction of flux measurements for density effects due to heat and water vapour transfer, *Quart. J. Roy. Meteor. Soc.*, **106**, 85–100, doi:10.1002/qj.49710644707.

Wilczak, J. M., S. P. Oncley, and S. A. Stage, 2001: Sonic anemometer tilt correction algorithms, *Bound.-Layer Meteor.*, **99**, 127–150.

Zhang, L. M., and Z. P. Shangguan 2002: Relationship between the soil moisture and the vegetation productivity in the Loess Plateau, *Arid Zone Res.* (in Chinese), **19**(4), 59–63.